iScience

CellPress

Article

Embryonic Crude Oil Exposure Impairs Growth and Lipid Allocation in a Keystone Arctic Forage Fish

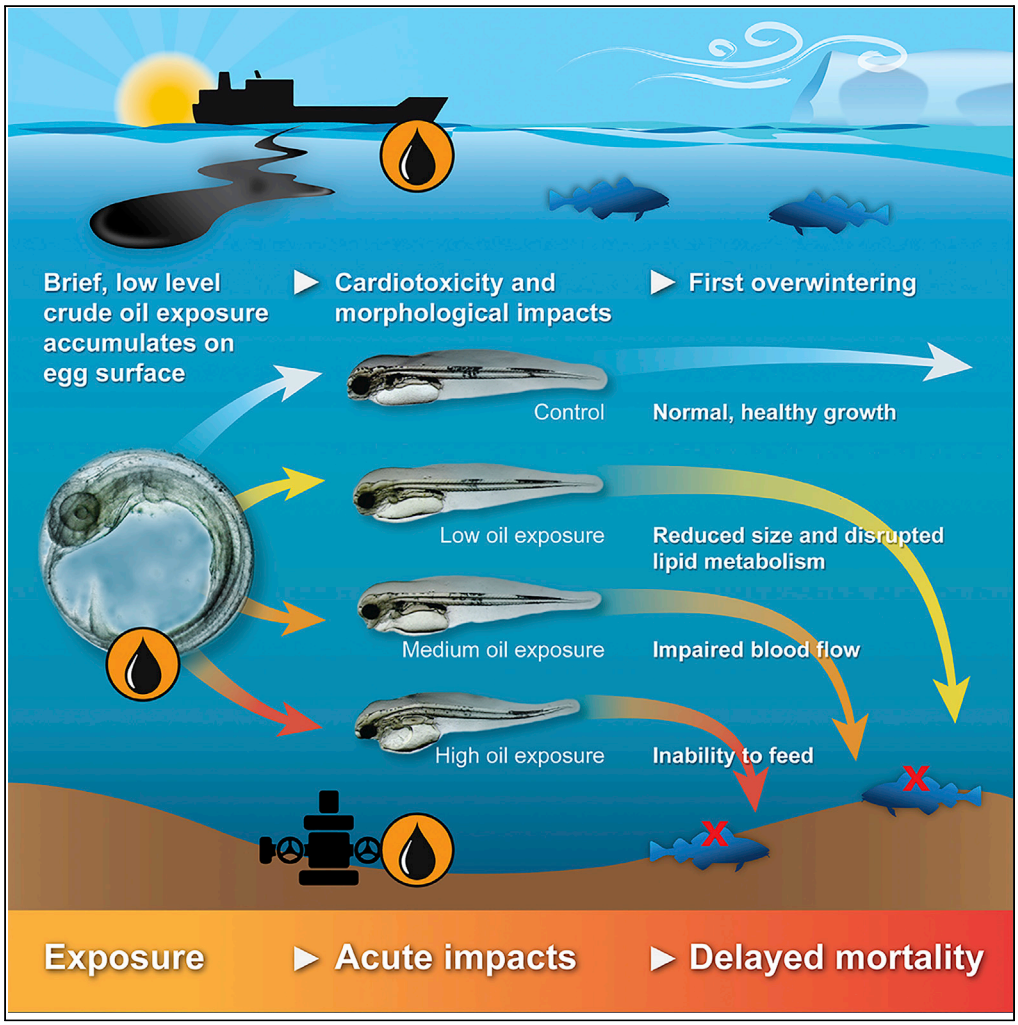

Benjamin J. Laurel, Louise A. Copeman, Paul Iseri, ..., Tiffany L. Linbo, Nathaniel L. Scholz, John P. Incardona

ben.laurel@noaa.gov

HIGHLIGHTS

Polar cod eggs are buoyant and accumulate crude oil droplets on the chorion

Crude oil disrupts embryonic cardiac function and larval lipid metabolism

Juvenile growth and lipid content are reduced following brief embryonic oil exposure

Polycyclic aromatic hydrocarbons are toxic to cod in parts per trillion concentrations

Laurel et al., iScience *19*, 1101–1113
September 27, 2019
https://doi.org/10.1016/j.isci.2019.08.051

iScience

CellPress

Article

Embryonic Crude Oil Exposure Impairs Growth and Lipid Allocation in a Keystone Arctic Forage Fish

Benjamin J. Laurel,[1,7,*] Louise A. Copeman,[2] Paul Iseri,[1] Mara L. Spencer,[1] Greg Hutchinson,[1] Trond Nordtug,[3] Carey E. Donald,[4] Sonnich Meier,[4] Sarah E. Allan,[5] Daryle T. Boyd,[6] Gina M. Ylitalo,[6] James R. Cameron,[6] Barbara L. French,[6] Tiffany L. Linbo,[6] Nathaniel L. Scholz,[6] and John P. Incardona[6]

SUMMARY

As Arctic ice recedes, future oil spills pose increasing risk to keystone species and the ecosystems they support. We show that Polar cod (*Boreogadus saida*), an energy-rich forage fish for marine mammals, seabirds, and other fish, are highly sensitive to developmental impacts of crude oil. Transient oil exposures ≥300 μg/L during mid-organogenesis disrupted the normal patterning of the jaw as well as the formation and function of the heart, in a manner expected to be lethal to post-hatch larvae. More importantly, we found that exposure to lower levels of oil caused a dysregulation of lipid metabolism and growth that persisted in morphologically normal juveniles. As lipid content is critical for overwinter survival and recruitment, we anticipate Polar cod losses following Arctic oil spills as a consequence of both near-term and delayed mortality. These losses will likely influence energy flow within Arctic food webs in ways that are as-yet poorly understood.

INTRODUCTION

Crude oil contains polycyclic aromatic hydrocarbons (PAHs) that are cardiotoxic. Three-ringed PAH families (e.g., phenanthrenes) enriched in crude oil block K^+ and Ca^{2+} ion conductances in cardiomyocytes, disrupting the normal rhythmic pumping of the heart (Brette et al., 2014, 2017). When this occurs in oil-exposed fish embryos, disruption of cardiac function leads to abnormal heart development (Incardona, 2017; Incardona and Scholz, 2016). Although cardiocirculatory defects alone would be sufficient to impact growth, more recent findings indicate that reduced cardiac function during embryonic and early larval development has other indirect effects that may be equally if not more consequential for individual fitness. Specifically, recent advances in RNA sequencing of oil-exposed Atlantic haddock (*Melanogrammus aeglefinus*) embryos identified alterations in the expression of genes involved in lipid metabolism (Sørhus et al., 2017). This suggests that disruption of bioenergetics during early development may be a prominent mechanism underlying latent impacts on fish growth and survival at later life stages.

Oil spill science in marine systems has thus far focused on fish species with distinct ecophysiological characteristics (Incardona and Scholz, 2016). This includes nearshore and pelagic species spawning in cold northern waters (Carls et al., 1999; Incardona et al., 2015) and rapidly developing sub-tropical species (Incardona and Scholz, 2018). In general, cold water species or those with strong cold tolerance are more sensitive to oil-induced toxicity (Edmunds et al., 2015; Incardona et al., 2014, 2015; Morris et al., 2018; Sørensen et al., 2017; Sørhus et al., 2016). Although common morphological and functional abnormalities are usually evident shortly after embryonic exposure, delayed reductions in growth and juvenile survival have been documented in pink salmon exposed to low concentrations of oil that did not cause externally visible malformation (Heintz, 2007; Heintz et al., 2000). These effects on growth could reflect a latent and lasting dysregulation of lipid metabolism. If so, this would have important consequences for global marine fisheries because management paradigms are premised on a positive relationship between juvenile bioenergetics and successful recruitment to adult populations (Bouchard et al., 2017; Copeman et al., 2017; Heintz et al., 2013).

Polar cod (*Boreogadus saida*) is a circumpolar species and one of the most abundant and important forage fish in Arctic ecosystems (Mueter et al., 2016). Significant changes in the distribution and abundance of cod would likely be highly disruptive to Arctic food webs, especially ice-obligate species (Bluhm and Gradinger,

[1]Alaska Fisheries Science Center, National Oceanic and Atmospheric Administration, Newport, OR, USA

[2]Oregon State University Hatfield Marine Science Center, Newport, OR, USA

[3]SINTEF Ocean, Trondheim, Norway

[4]Institute of Marine Research, Bergen, Norway

[5]National Oceanic and Atmospheric Administration, Office of Response and Restoration, Anchorage, AK, USA

[6]Northwest Fisheries Science Center, National Oceanic and Atmospheric Administration, Seattle, WA, USA

[7]Lead Contact

*Correspondence: ben.laurel@noaa.gov

https://doi.org/10.1016/j.isci.2019.08.051

2008; Choy et al., 2017; Vihtakari et al., 2018). Polar cod embryos exposed to a water-soluble fraction of crude oil from oiled gravel columns showed reduced hatching success and increased frequencies of malformations at very low total (∑)PAH concentrations (≤1 μg/L) (Nahrgang et al., 2016). In the present study we exposed Polar cod embryos using an environmentally realistic oil dispersion and investigated the latent consequences for two critical survival periods. These included "first-feeding success," wherein newly hatched larvae consume their yolk reserves and begin feeding (Houde, 2008; Laurel et al., 2011), and "overwintering success," a process that is critically dependent on the size-at-age and energy density (lipid) of juvenile fish entering their first winter (Copeman et al., 2008; Siddon et al., 2013; Sogard and Olla, 2000). To emulate environmentally realistic post-spill oil exposures, relatively low levels of oil droplets were generated using a previously described dispersion system (Nordtug et al., 2011), with nominal oil loadings (by mass) of 100, 300, and 900 μg/L. Dispersed oil was released into exposure tanks for only 3 days of the ~40-day embryonic development period, during mid-embryogenesis after the heart first began beating (20 days post-fertilization, dpf; Figure S1). Embryos were then transferred to new vessels and incubated in clean seawater to hatch (from 27–50 dpf) before a final transfer to flow-through tanks supplied with live prey for grow-out (to 193 dpf). We describe the toxicity of crude oil to the developing heart and craniofacial structures of cod embryos. We also characterize how trace and transient embryonic oil exposures affect growth rate and lipid content at later life stages.

RESULTS

Buoyancy of Polar Cod Embryos Enhances Exposure to Dispersed Oil

Oil droplets rose to the surface to form slicks within the first 24 h of oil release. During a subsequent 4-day washout with clean seawater, buoyant embryos remained in the exposure tanks, in contact with the surface oil as it dissipated. To characterize exposure chemically, PAHs were measured in exposure water collected directly from the tank inlets at the exposure start (day 0) and day 1 and from the water column at exposure days 1, 3, and 7 (Table S1; Data S1). To determine any potential increase in exposure from contact with the surface slick, embryos were also placed in 500-μm mesh chambers (which allowed passage of dispersed oil droplets) in the water column below the slick. Tissue concentrations of PAHs and levels of PAH-induced *cyp1a* mRNA were measured in both submerged and floating, surface-oriented embryos (overall experimental design shown in Figure S1).

Over the 3 days of oil release, $\sum PAH_{42}$ concentrations in the water column (Table 1) ranged from 0.65 ± 0.20 to 1.1 ± 0.1 μg/L for the low concentration (100 μg/L oil load), 2.6 ± 0.3 to 4.0 ± 0.1 μg/L for the medium concentration (300 μg/L oil load), and 11.9 ± 2.3 to 18.3 ± 2.7 μg/L for the high concentration (900 μg/L oil load). Control seawater contained very low background levels of PAHs (0.11 μg/L; Table 1). Visual inspection of embryos floating at the surface showed oil droplets adhering to the chorions (eggshell) within the first 24 h of oil release, with sufficient binding to remain attached through collection and transfer into methylcellulose for microscopic imaging (Figure S2). By day 3 of oil release, droplets were observed on chorions at even the low exposure concentration, with continued accumulation at the higher concentrations (Figure 1). Consequently, measurements of embryo-associated PAHs were conducted separately for floating embryos to compare with artificially submerged embryos to elucidate effects of direct contact with surface slicks (Table 1; Data S1). By exposure day 3, the ∑PAH in submerged embryos ranged from 67 ± 7 to 832 ± 85 ng/g wet weight and in floating embryos from 517 ± 94 to 4195 ± 650 ng/g. This represented an increase of 8, 9, and 5 times at the low, medium, and high exposure concentrations, respectively. We also measured tissue PAHs after oil release was stopped and embryos remained in contact with the dissipating surface slicks (Table 1; exposure day 7). Although embryo-associated ∑PAH had declined for the low and medium exposures (284 ± 100 and 4259 ± 937 pg/embryo, respectively), ∑PAH continued to rise for the high dose (11,343 ± 1898 pg/embryo). After 4 days incubation in clean seawater, tissue ∑PAH levels dropped by about 75% for all doses, consistent with metabolic depuration (Table 1).

Levels of *cyp1a* mRNA reflect a response to cell-internal PAHs within tissues. Therefore, quantitative measures of *cyp1a* induction can distinguish the internalized bioavailable fraction of PAHs from external PAHs retained in oil droplets adhering to the chorion. Using fold-change relative to controls, *cyp1a* induction was linear in submerged embryos but non-linear and approaching saturation in floating embryos (Figure S3). Estimated true internal PAH concentrations were calculated for floating embryos by interpolation using the linear equation for submerged embryo *cyp1a* induction (Table 1). This demonstrated that surface slick exposure and oil droplet binding to the chorion led to increased PAH uptake in floating embryos. Based on

Nominal Oil Loading	Water Column Total ∑PAH[a] (μg/L)	Egg Incubation Position	Day 3 Tissue ∑PAH (ng/g Wet Weight)	Day 3 Tissue ∑PAH (pg/Embryo)	*cyp1a* mRNA Induction (Fold Change)	Interpolated Day 3 Tissue ∑PAH (pg/Embryo)[b]	Percent Day 3 ∑PAH Bioavailable	Day 7 Tissue ∑PAH (pg/Embryo)	4 Days Post-exposure Tissue ∑PAH (pg/Embryo)	Percent Depurated 4 Days Post Exposure
0	0.11 ± 0.03	Floating	43 ± 21	102 ± 50	0.78 ± 0.15			13 ± 7	28 ± 5	
		Submerged	17 ± 2	40 ± 5	1.3 ± 0.2					
100 μg/L	1.1 ± 0.1	Floating	517 ± 94	1,232 ± 223	62 ± 11	1,378	100	284 ± 100	81 ± 18	72
		Submerged	67 ± 7	161 ± 17	11 ± 3					
300 μg/L	4.0 ± 0.1	Floating	2,358 ± 390	5,448 ± 901	69 ± 10	1,529	28	4,259 ± 937	973 ± 214	77
		Submerged	272 ± 89	629 ± 206	30 ± 12					
900 μg/L	18.3 ± 2.7	Floating	4,195 ± 650	9,858 ± 1,527	115 ± 9	2,565	26	11,343 ± 1,898	2,864 ± 362	75
		Submerged	832 ± 85	1,956 ± 210	88 ± 14					

Table 1. Quantification of Exposure by Measures of Water and Embryo $\sum PAH_{42}$ and *cyp1a* mRNA Induction

Tissue concentrations are means (±SEM) of samples from four replicate tanks.

[a]Measured at exposure day 3.

[b]Calculated from the linear equation relating measured ∑PAH to *cyp1a* mRNA induction in submerged embryos (Figure S3).

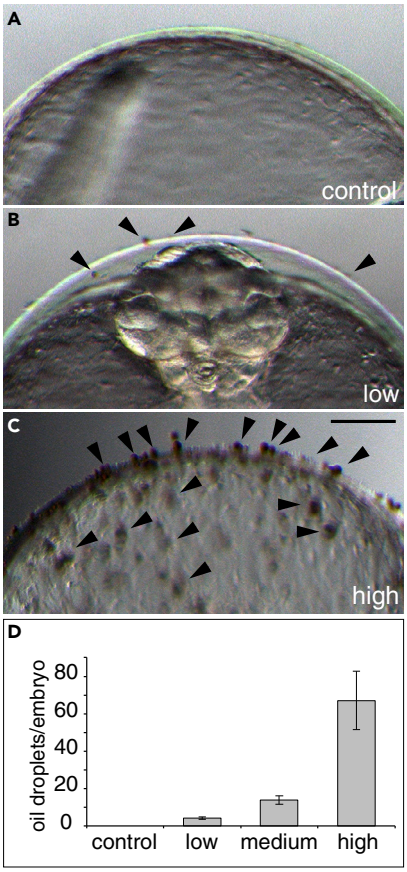

Figure 1. Oil Droplets Bind to the Polar Cod Chorion

(A–C) Higher-magnification views compare embryos from the control surface (A) and low (B) and high (C) exposures on the day of transfer to clean water.

(D) Quantification of adhered droplets (mean ± S.E.M.) from representative images of single embryos (4 per replicate, 16 total per treatment) at exposure day 3 (end of oil release into the water column).

Arrowheads indicate oil microdroplets. Scale bar is 200 μm.

the levels of *cyp1a* induction, contact with surface oil increased the internal concentration of ∑PAH 8.6 times for the low oil load and 2.4 times for the medium load, and 1.3 times for the high oil load (Table 1). At the low oil load, this means that 100% of the measured embryo-associated PAH was bioavailable, whereas roughly 25%–30% was bioavailable at the higher loads. These findings demonstrate that even small oil spills can have outsized impact for highly buoyant Polar cod eggs through the formation of surface slicks. For simplicity and consistency in referring to oil concentrations, hereafter, toxicity endpoints in floating embryos (below) are simply related to "low," "medium," and "high" exposures based on *cyp1a*-based ("true") internal concentrations.

Transient Exposure during Mid-organogenesis Is Sufficient to Produce Latent Cardiac and Craniofacial Defects

At the end of exposure (27 dpf), embryos displayed dose-dependent slowing of the heart rate (bradycardia; Figure 2A, bottom line) and an increase in frequency of abnormal heart rhythms (Figure 2B). Measuring atrial contractions in digital videos showed that the duration between heartbeats increased in a dose-dependent manner from 3.0 ± 0.1 to 4.0 ± 0.2 s/beat (Figure 2B, top line) and that at a relatively sharp dose threshold, interbeat duration became irregular (atrial fibrillation) (Figure 2B, bottom line; Figures 2C–2F). Many individuals at the high dose showed, in addition to irregular rate, retrograde conduction from the atrioventricular junction (Video S1). Cardiac function was assessed again in hatching stage yolk-sac larvae at 42 dpf. Despite likely depuration of PAHs over the intermittent 15 days in clean water, larvae displayed a persistent dose-dependent bradycardia (Figure 2A, top line) but no rhythm irregularities.

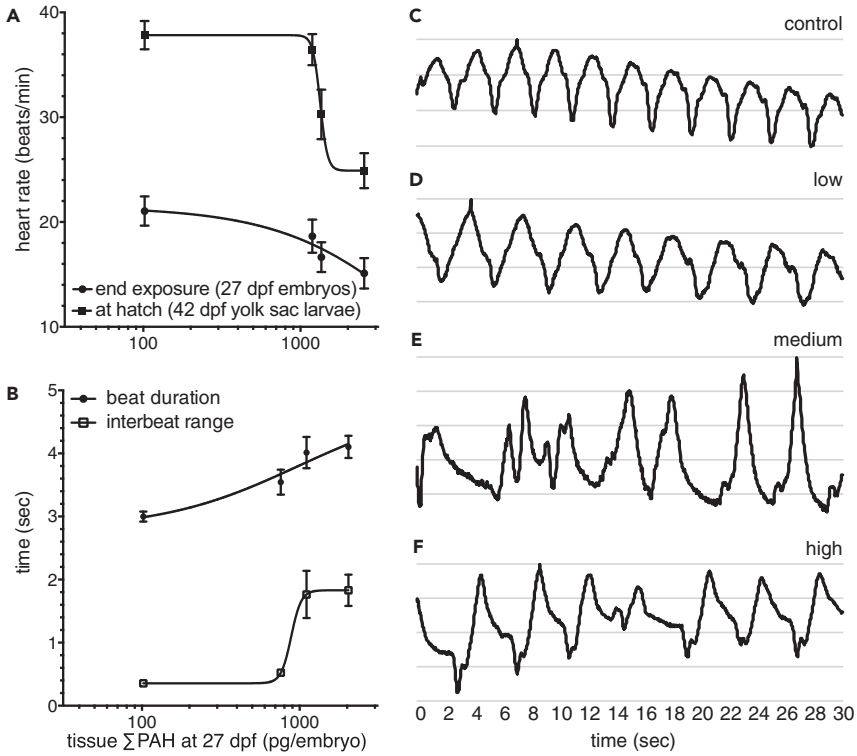

Figure 2. Cardiac Dysfunction Immediately Following Embryonic Oil Exposure

(A) Dose-dependent reduction of heart rate measured at the end of exposure (lower line) and at hatch after 15 days in clean seawater (upper line).

(B) Dose-dependent increases in heartbeat duration (upper line) and irregularity (lower line) measured at the end of exposure.

(C–F) Graphical representations of heart rhythms derived from digital videos, used to generate data shown in (B). Wave forms represent atrial motion; baselines drift because of embryo movement during video acquisition.

Values are means (±SEM) from end of exposure (A, bottom line, and B) and are based on video analyses of 10 representative embryos per replicate tank (n = 4 replicates per treatment) and 30 larvae per tank at hatch.

Consistent with a reduction in cardiac output, larvae accumulated pericardial and yolk sac edema. Edema was dose-dependent in severity, quantified by scoring contact between the cardiac chambers and pericardial membrane in lateral view digital videos (Figure 3A). Because the tissue PAH depuration data indicate a half-life of $\lesssim$ 3 days, PAHs were most likely nearly completely eliminated by this point. Therefore, the persistent bradycardia likely reflects electrophysiological remodeling of cardiomyocytes in response to oil exposure, rather than acute impacts on ion conductances.

The effects of oil exposure on overall gross morphology of yolk sac larvae were remarkably similar to those observed in other closely related gadids, Atlantic haddock (*Melanogrammus aeglefinus*) and Atlantic cod (*Gadus morhua*) (Figure S4). Polar cod larvae showed craniofacial defects, characterized by a loss of jaw structures progressing from the upper jaw/basal neurocranium to the lower jaw with increasing dose (Figure 3B). Although not quantified, an apparent reduction in melanophore pigment cells at the high dose was noted (Figure S4D). There was reduced hatch success; in addition, oil-exposed embryos were significantly smaller at hatch (standard length) and had proportionately smaller eyes (Figures 4A–4C). Other structures and metrics (e.g., myotome depth) were not affected (Figure 4D).

Embryonic Oil Exposure Leads to Persistent Derangements in Larval-Juvenile Lipid Metabolism, Even in Morphologically Normal Survivors

Surviving larvae exposed to oil also experienced higher rates of abnormalities that would likely impair swimming and foraging ability, including the fluid imbalance represented by pericardial and yolk sac edema, axial deformation, and jaw deformities (e.g., Figure S4). We therefore monitored survival and

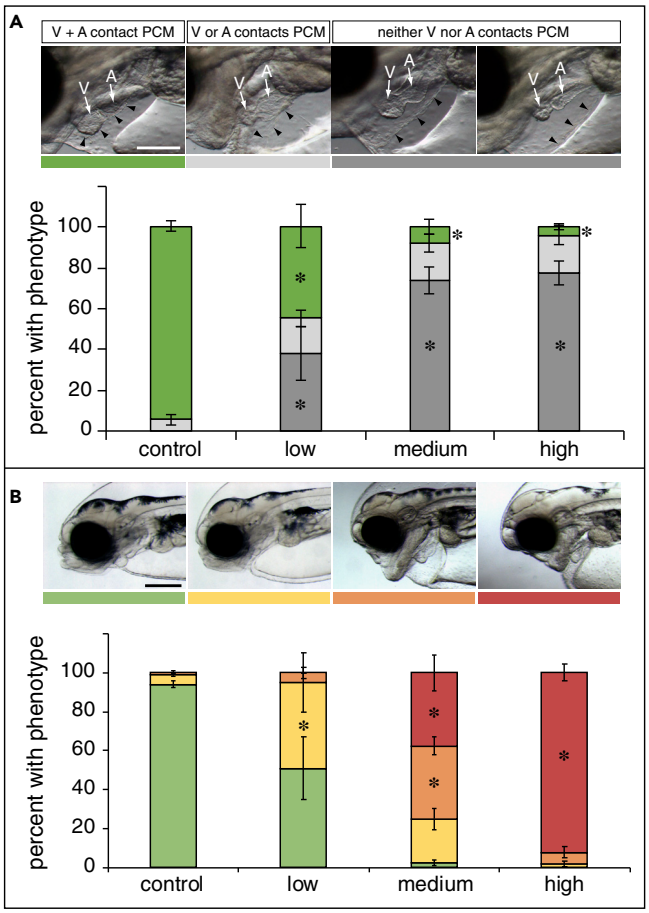

Figure 3. Quantification of Pericardial Edema and Craniofacial Malformation in Post-hatch (Yolk Sac) Larvae

(A) Representative images at top show criteria for scoring presence of pericardial edema by contact of the ventricular (*V*) or atrial (*A*) chambers with the pericardial membrane (*PCM*, arrowheads). Edema was scored as present if one chamber did not contact the pericardial membrane (gray and dark gray; green, no edema). Scale bar is 200 μm. Plot values are means (±SEM) for the three categories based on multiple larvae (n = 30) from each replicate (n = 4) for each treatment.

(B) Representative images at top show categorization of craniofacial defects as mild (yellow), moderate (orange), or severe (red) based on loss of anterior jaw structures. Values are means (±SEM) based on imaging for 30 representative individuals per replicate tank (n = 4 replicates per treatment). Scale bar is 400 μm.

Asterisks in both indicate $p < 0.01$ for post hoc means comparison with control by Dunnett's Test following ANOVA.

growth after yolk sac larvae were placed on a previously established dietary regimen (Koenker et al., 2018). To profile changes in bioenergetics, lipid classes were measured throughout the experiment, beginning with embryonic exposure. Lipids were subsequently measured in newly hatched yolk sac larvae, through larval growth, and in juveniles. In addition, further latent effects on cardiac morphology and function were assessed.

By 86 dpf (43 days post hatch), there were no fish surviving from the high-exposure treatment. Fish from the low- and medium-exposure groups still displayed cardiac defects (Figure S5) despite surviving at relatively high numbers (albeit significantly lower than control groups, $p < 0.001$). Although there was a slight decreasing trend in the size of the ventricle, this was not significant when normalized to standard length among controls (Figure S5D). However, there was a significant dose-dependent reduction in the ventricular aspect ratio, indicating a relationship between oil exposure and rounder ventricles. In addition, oil-exposed larvae had reduced trabeculation (Figure S5C). Although neither normalized ventricular size nor heart rate were different at this point, oil-exposed larvae showed persistent dose-dependent edema, likely evidence of reduced cardiac output (Figure S6).

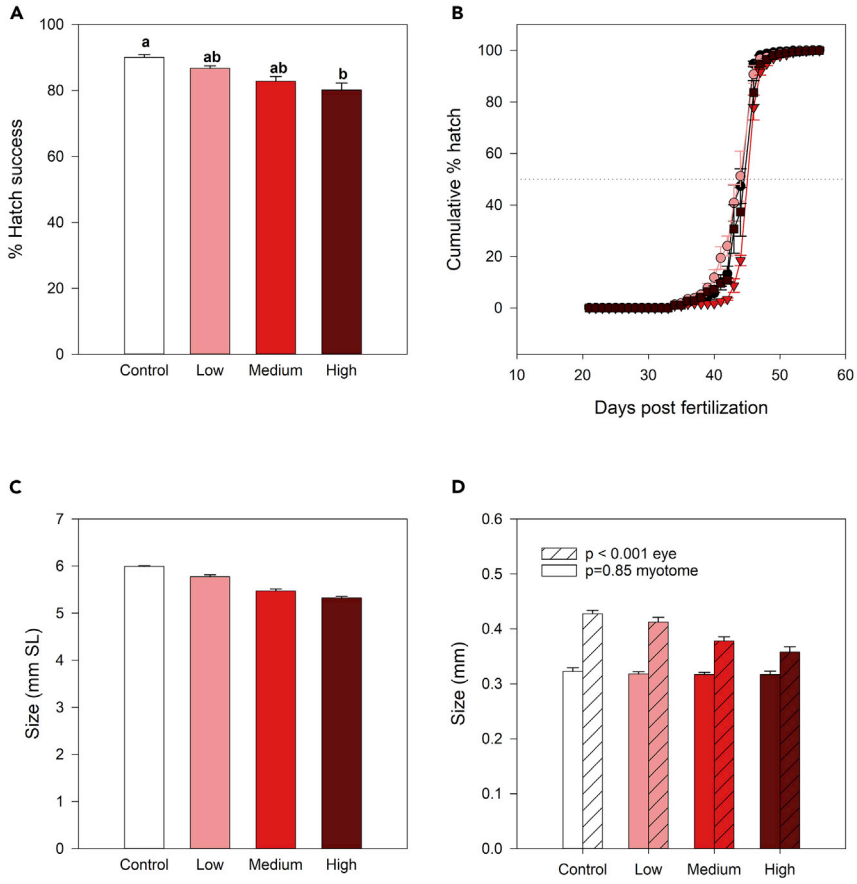

Figure 4. Acute Extracardiac Impacts of Oil Exposure on Polar Cod Embryos

Increasing oil exposure decreased hatching success (A) but had no significant effect on cumulative hatch rate (B). The size of cod larvae at hatch (C) and eye diameter (D) decreased with oil exposure, whereas body depth (myotome) remained constant (D). Values are means (±SEM) of total counts per replicate tank (A and B) or 20 individuals/tank (C and D). Letters indicate statistically different groups determined by ANOVA with Tukey-Kramer HSD test for post hoc means comparisons.

Although 100% of the medium-exposure group showed edema at this stage, 65% of larvae exposed to the low dose were grossly normal.

Relationships between morphology, physiological function (e.g., fluid balance), metabolism, growth, and survival were revealed by repeated sampling over the next ~150 days. Lipid class profiling demonstrated prolonged impacts on lipid metabolism that changed in character from the initial rapid larval growth stage to post-metamorphic juveniles. Although lipid classes in embryos were not different across treatments at the end of the transient oil exposure (Figure 5A), at hatch oil-exposed yolk sac larvae had elevated levels of three lipid classes on a per-dry weight basis; triacylglycerols (TAGs), free fatty acids (FFAs), and sterols (STs). Throughout feeding stages, the latent impacts of embryonic oil exposure were observable in larvae and juveniles by way of poor survival, altered lipid content (shown for TAGs and normalized to dry weight), and decreased growth (Figures 4B and 4C). By 66 dpf, relative elevations of TAGs in oil-exposed larvae became exacerbated, with the high-dose larvae showing little change in TAG content over the preceding 20 days, remaining 3.7 times higher than controls (Figure 5C). By 87 dpf, as animals completely shifted to exogenous feeding, no high-dose fish survived and TAG levels were at their lowest but not significantly different among the control and remaining oil-exposed groups. By 123 dpf, all larvae in the medium-exposure group were dead. Presumably, fish in the high- and medium-dose groups succumbed to sequelae stemming from severe fluid imbalance represented by persistent edema. In contrast, large numbers of larvae from the control and low (100 μg/L) exposures completed flexion and survived into the juvenile stage. At this point (123 dpf), both control and oil-exposed (low-dose) fish were at pre-flexion stage and

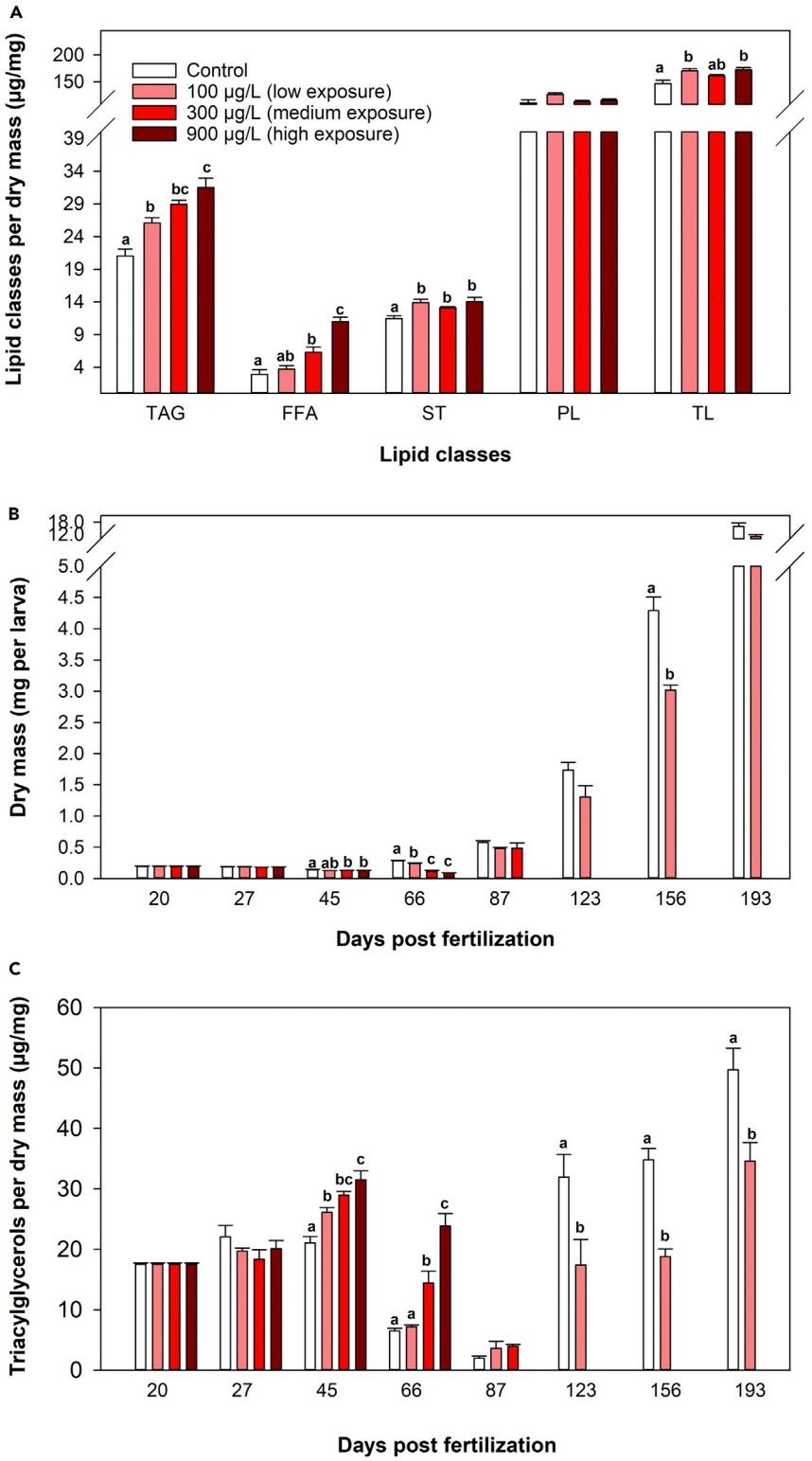

Figure 5. Latent (Delayed in Time) Impacts of Embryonic Oil Exposure on Polar Cod

(A) Newly hatched larvae exposed to oil had elevated Triacylglycerol (TAG), Free Fatty Acids (FFA), and Total Lipids (TL), but there was no significant difference in Sterols (ST) or Polar Lipids (PL) classes among treatments.

Figure 5. *Continued*

(B) The dry mass of surviving larvae transiently exposed to oil as embryos was significantly lower than controls between 66 and 156 days post fertilization (dpf).

(C) The lipid density (triacylglycerol, TAG) of oil-exposed embryos was initially higher during the larval period (hatch to flexion; 45 and 67 dpf) but was lower in oil-exposed fish during the juvenile period (123–193 dpf). Dry mass and lipid density values are means (±SEM) per fish based on replicate pooled or individual fish depending on the time of sampling (see Transparent Methods). Letters indicate statistically different groups determined by ANOVA with Tukey-Kramer HSD test for post hoc means comparisons.

showed evidence of TAG accumulation (Figure 5C), but exposed fish showed significantly lower levels. Compared with controls, low-dose survivors had 46% less TAG at 123 dpf, 46% less TAG at 156 dpf (flexion stage), and 31% less TAG by termination of the experiment at 193 dpf, at which point fish had transformed into early juveniles. Importantly, animals that survived oil exposure were significantly smaller than unexposed controls at the 123 and 156 dpf time points, but were not different in dry weight by 193 dpf, despite having a lower TAG content (Figure 5B).

DISCUSSION

Vulnerability of Polar Cod to Low-Level Exposure from Oil Spills

These findings have two key sets of implications. First, they have broad implications for understanding the long-term impact of oil spills on fish populations. Second, they have discrete and important implications for the vulnerability of Polar cod to spills in the Arctic. Studies conducted 20 years ago in the wake of the Exxon Valdez oil spill demonstrated that embryonic exposure to oil at levels insufficient to produce malformed larvae nevertheless led to reduced juvenile growth and marine survival (Heintz, 2007; Heintz et al., 2000). For pink salmon, these effects explained population-level impacts observed on the scale of individual streams in oiled habitat (Peterson et al., 2003; Rice et al., 2001). Although the effects of early exposure on later growth and survival have been presumed to be connected to developmental impacts on the heart, the precise mechanisms have remained elusive. Lipids are essential for both growth and early survival in marine fish larvae (Tocher, 2003), even more critically so at the extremely cold temperatures occupied by Polar cod (Copeman et al., 2017). Thus, the profound changes in lipid composition and dynamics observed here in Polar cod represent a probable mechanism for reduced growth and survival.

Owing to several life history characteristics, we anticipate Polar cod will be particularly vulnerable to future oil spills. First, as noted earlier, crude oil is relatively more toxic to cold water fishes. Second, their highly buoyant embryos (Laurel et al., 2018) make exposure to oil in surface slicks much more likely. Third, the adherence and accumulation of oil micro-droplets on the outside of the chorion suggests that even short-term contact with a slick could lead to a localized and prolonged release of dissolved PAHs. Consistent with the above, acute effects of spilled oil were magnified in Polar cod embryos, as evidenced by a higher *cyp1a* induction in embryos floating near the surface slick relative to those caged below in the water column. This effect was highly magnified at the lowest levels of dispersed oil released into the water column. Therefore, the transport and fate of oil in Arctic environments potentiates the exposure risk for Polar cod. Oil weathers more slowly in colder water and can be encapsulated in sea ice as it forms, suspending weathering and degradation until the oil is released during breakup. Oil is likely to accumulate and persist along the margins, in openings, and under sea ice, all rearing habitats for Polar cod embryos and larvae. Finally, the general importance of lipids to multiple aspects of fish early history stages, compounded by the special role of lipids in Polar cod, only increases this species' sensitivity.

Implications of Deranged Lipid Metabolism for Early Growth and First-Year Survival

In the natural environment, high amounts of TAGs can improve first-feeding success by reducing starvation risk during the transition from endogenous yolk-sac-based energy to the exogenous feeding stage (Laurel et al., 2008). Although TAGs and FFAs were significantly higher in animals exposed to the medium and high oil doses, the availability of these increased energy stores for metabolic activity is uncertain. Earlier studies on Atlantic haddock indicate oil exposure may interfere with the ability of larvae to mobilize lipids from the yolk during the critical transition from endogenous to exogenous feeding. Specifically, genetic upregulation of genes controlling intrinsic cholesterol and lipid biosynthesis and transport has been postulated to reflect deprivation in larval tissues as a consequence of the heart and circulatory system failing to deliver lipoproteins from the yolk (embryos) and intestine (larvae) (Sørhus et al., 2017). Our lipid results are from

whole larval lipid pools, and the elevation of TAG, FFA, and ST in exposed larvae likely reflect both an upregulation of lipid synthesis in larval tissues as well as under-utilization of yolk lipids.

Higher concentrations of lipid in larval tissues has also previously manifested in histological findings such as liver lesions that have been measured in cultured fish both as a result of excessive fat storage or from exposure to hydrocarbons (Agamy, 2012). Furthermore, increased presence of FFAs are more indicative of fish stress (Mazeaud et al., 1977), and FFAs are generally not found in high levels in fish tissues except as a result of sample degradation (Parrish, 1988). The pairing of these acute findings of lipid metabolic disorder with other measures of larval physiology, morphology, and survival provide strong evidence that lipid synthesis genes are promising indicators, or biomarkers, for injury in fish embryos exposed to crude oils (Sørhus et al., 2017).

After flexion, surviving oil-exposed fish with poor cardiac function may have begun the juvenile phase with an energetic deficit, necessitating increased TAG utilization for compensatory growth and maintenance while leaving proportionally less TAG for storage in advance of the first winter. Basal metabolic processes in larvae are stage-specific (Peck and Moyano, 2016), and shifts in TAG levels can indicate a reduced use of TAG stored in yolk, the *de novo* synthesis of TAG in embryonic tissues deprived of yolk from the circulation, or both.

The observed changes in growth and lipid content can be expected to directly impact the health and survival of individual cod and by extension, recruitment into forage fish populations that support the upper trophic levels of Polar food webs (Hop and Gjosaeter, 2013). Biological productivity at high latitudes supports large stocks of fish and mammals and is driven by a highly specialized lipid-based energy transfer system (Falk-Petersen et al., 1990, 2009). Gadids in the higher Arctic are also reliant on sufficient lipid stores to survive the relatively longer period of overwintering (Copeman et al., 2017). For example, walleye pollock (*G. chalcogrammus*) in the Eastern Bering Sea represent one of the largest single species fisheries in the world. Survival through their first winter is strongly correlated with their energetic content at the beginning of fall and their eventual recruitment to the fishery 2–3 years later (Heintz et al., 2013). The ability to successfully forage and allocate energy to satisfy immediate demands for growth, as well as storage needs to offset future winter starvation stress, is a particularly challenging trade-off for juveniles facing size-dependent predation in their first year (Sogard, 1997). Many of the fish in the low-exposure treatment, with a ~25%–30% reduction in size and TAG density, would unlikely have sufficient reserves to successfully overwinter. Latent effects of oil exposure on individual survival and productivity and resulting impacts on fish populations and ecosystems should be incorporated into prospective risk assessments and retrospective injury assessments. However, projections of Polar cod losses following large oil spills will also need to consider other population drivers, including thermal habitat conditions, prey availability and quality, and top-down predation pressures (Brodersen et al., 2011).

Potential Interactions of Oil Exposure with Other Environmental Stressors in the Arctic

Importantly, the adverse health effects we report here are likely to be exacerbated by parallel environmental stressors in Arctic habitats. Among the latter, most notable are increasing seawater temperatures and co-exposure to UV radiation in natural sunlight. Polar cod embryos and larvae are highly sensitive to temperature (Koenker et al., 2018; Laurel et al., 2016), and thermal stress may potentiate oil toxicity in this species. Atmospheric warming is occurring at a more rapid rate in the Arctic than in temperate zones, and observational data indicate that ocean surface temperatures are increasing in every polar region (e.g., 0.5°C per decade in the Chukchi Sea [Timmermans and Proschutinsky, 2014]). These changes in atmospheric warming are driving the loss of Arctic sea ice (Jeffries et al., 2018). As a result, the area is much more accessible to shipping and oil exploration/extraction, which then increases the risk of oil spills (Foster et al., 2015). Lastly, the photoactivation of chemicals in crude oil and the bunker oils that currently fuel large vessels is well known to increase lethal toxicity to fish early life stages (Barron et al., 2003; Incardona et al., 2012). This will be a particularly important hazard for translucent and buoyant organisms that are within the zone of UV penetration in the upper water column, i.e., Polar cod.

Finally, as it relates to the potential oiling of cod spawning habitats, the response of fish in our low treatment (~1 μg/L water column $\sum$PAHs) indicates that individual PAHs are toxic in the parts-per-trillion concentration range. Although this very low exposure did not cause significant mortality through larval development, it was sufficient to disrupt embryonic cardiac function and produce a lasting dysregulation of lipid homeostasis well into the juvenile life stage. This latent form of injury to cod suggests that the toxic footprint of any future Arctic spills will be much larger in space and time than previously anticipated.

Limitations of the Study

The current study addresses vulnerability at one particular life stage, which has proven to be particularly sensitive in northern temperate species. The adherence of droplets to the egg chorion along with the long embryonic development times of Polar cod will likely result in exposure risks beyond what was measured. Population- and ecosystem-level impacts from laboratory studies are also difficult to predict, and the current study is unable to quantify injury level beyond the individual. Multi-stressors such as temperature and UV exposure may amplify the RNA-seq and phenotypic effects observed in the study. Mortality rates in larval fish are also largely driven by prey availability and predation, which would likely exacerbate mortality rates observed in the oil-exposed embryos due to unmeasured physiology, e.g., impairments to visual acuity and swim performance. Finally, although there was significant effort to simulate *in situ* oil exposure by way of a micro-droplet generator, this study does not account for complex ice dynamics and turbulence that may result in different exposure scenarios.

METHODS

All methods can be found in the accompanying Transparent Methods supplemental file.

SUPPLEMENTAL INFORMATION

Supplemental Information can be found online at https://doi.org/10.1016/j.isci.2019.08.051.

ACKNOWLEDGMENTS

We thank S. Haines, M. Ottmar, and the NOAA Alaska Fisheries Science Center staff in Newport, Oregon, for the laboratory setup, live-food culture and husbandry of Polar cod. We also appreciate support from M. Stowell at the Marine Lipid laboratory at the Hatfield Marine Science Center and the staff in the Environmental Chemistry Program at the Northwest Fisheries Science Center. C. Ryer and D. Baldwin contributed to the study design. E. Mudrock assisted with live imaging for cardiac and craniofacial defects, and K. Peck helped with primer design for qPCR assays. Thanks to P. Irvin for the illustration and assistance in the design of the graphical abstract. This study was partially funded by NOAA's Office of Response and Restoration (Assessment and Restoration Division) and the Oil Spill Recovery Institute. Thanks to L. Rogers and J. Napp for providing constructive feedback on earlier versions of this manuscript.

AUTHOR CONTRIBUTIONS

B.J.L., L.A.C., S.M., S.E.A., N.L.S., and J.P.I. participated in the conception and design of the research. T.N., P.I., and G.H. assisted with design and setup of oil exposure and live fish culture system. B.J.L., L.A.C., P.I., M.L.S., G.H., T.L.L., B.L.F., and J.P.I. assisted in the execution of experiments. B.J.L., L.A.C., C.E.D., S.M., D.T.B., G.M.Y., J.R.C., T.L.L., and J.P.I. analyzed data. B.J.L., L.A.C., N.L.S., and J.P.I. performed statistical analyses and interpreted the results of the experiment. B.J.L., L.A.C., N.L.S., and J.P.I. prepared figures and drafted the manuscript. All authors edited and reviewed the manuscript.

DECLARATION OF INTERESTS

The authors declare no competing interests.

Received: April 12, 2019
Revised: July 8, 2019
Accepted: August 27, 2019
Published: September 27, 2019

REFERENCES

Agamy, E. (2012). Histopathological changes in the livers of rabbit fish (*Siganus canaliculatus*) following exposure to crude oil and dispersed oil. Toxicol. Pathol. *40*, 1128–1140.

Barron, M.G., Carls, M.G., Short, J.W., and Rice, S.D. (2003). Photoenhanced toxicity of aqueous phase and chemically dispersed weathered Alaska North Slope crude oil to Pacific herring eggs and larvae. Environ. Toxicol. Chem. *22*, 650–660.

Bluhm, B.A., and Gradinger, R. (2008). Regional variability in food availability for arctic marine mammals. Ecol. Appl. *18*, 77–96.

Bouchard, C., Geoffroy, M., LeBlanc, M., Majewski, A., Gauthier, S., Walkusz, W., Reist, J.D., and Fortier, L. (2017). Climate warming enhances polar cod recruitment, at least transiently. Prog. Oceanogr. *156*, 121–129.

Brette, F., Machado, B., Cros, C., Incardona, J.P., Scholz, N.L., and Block, B.A. (2014). Crude oil impairs cardiac excitation-contraction coupling in fish. Science *343*, 772–776.

Brette, F., Shiels, H.A., Galli, G.L.J., Cros, C., Incardona, J.P., Scholz, N.L., and Block, B.A.

(2017). A novel cardiotoxic mechanism for a pervasive global pollutant. Sci. Rep. *7*, 41476.

Brodersen, J., Rodriguez-Gil, J.L., Jonsson, M., Hansson, L.A., Bronmark, C., Nilsson, P.A., Nicolle, A., and Berglund, O. (2011). Temperature and resource availability may interactively affect over-wintering success of juvenile fish in a changing climate. PLoS One *6*, e24022.

Carls, M.G., Rice, S.D., and Hose, J.E. (1999). Sensitivity of fish embryos to weathered crude oil: Part I. Low-level exposure during incubation causes malformations, genetic damage, and mortality in larval Pacific herring (*Clupea pallasi*). Environ. Toxicol. Chem. *18*, 481–493.

Choy, E.S., Rosenberg, B., Roth, J.D., and Loseto, L.L. (2017). Inter-annual variation in environmental factors affect the prey and body condition of beluga whales in the eastern Beaufort Sea. Mar. Ecol. Prog. Ser. *579*, 213–225.

Copeman, L.A., Laurel, B.J., Spencer, M., and Sremba, A. (2017). Temperature impacts on lipid allocation among juvenile gadid species at the Pacific Arctic-Boreal interface: an experimental laboratory approach. Mar. Ecol. Prog. Ser. *566*, 183–198.

Copeman, L.A., Parrish, C.C., Gregory, R.S., and Wells, J.S. (2008). Decreased lipid storage in juvenile Atlantic cod (*Gadus morhua*) during settlement in cold-water eelgrass habitat. Mar. Biol. *154*, 823–832.

Edmunds, R.C., Gill, J.A., Baldwin, D.H., Linbo, T.L., French, B.L., Brown, T.L., Esbaugh, A.J., Mager, E.M., Stieglitz, J.D., Hoenig, R., et al. (2015). Corresponding morphological and molecular indicators of crude oil toxicity to the developing hearts of mahi mahi. Sci. Rep. *5*, 17326.

Falk-Petersen, S., Hopkins, C., and Sargent, J. (1990). Trophic Relationships in the Pelagic, Arctic Food Web. Trophic Relationships in the Marine Environment (Aberdeen University Press), pp. 315–333.

Falk-Petersen, S., Mayzaud, P., Kattner, G., and Sargent, J. (2009). Lipids and life strategy of Arctic Calanus. Mar. Biol. Res. *5*, 18–39.

Foster, K.L., Stern, G.A., Carrie, J., Bailey, J.N.-L., Outridge, P.M., Sanei, H., and Macdonald, R.W. (2015). Spatial, temporal, and source variations of hydrocarbons in marine sediments from Baffin Bay, Eastern Canadian Arctic. Sci. Total Environ. *506*, 430–443.

Heintz, R.A. (2007). Chronic exposure to polynuclear aromatic hydrocarbons in natal habitats leads to decreased equilibrium size, growth, and stability of pink salmon populations. Integr. Environ. Assess. Manag. *3*, 351–363.

Heintz, R.A., Rice, S.D., Wertheimer, A.C., Bradshaw, R.F., Thrower, F.P., Joyce, F., and Short, J.W. (2000). Delayed effects on growth and marine survival of pink salmon *Oncorhynchus gorbuscha* after exposure to crude oil during embryonic development. Mar. Ecol. Prog. Ser. *208*, 205–216.

Heintz, R.A., Siddon, E.C., Farley, E.V., and Napp, J.M. (2013). Correlation between recruitment and fall condition of age-0 pollock (*Theragra chalcogramma*) from the eastern Bering Sea under varying climate conditions. Deep Sea Res. II *94*, 150–156.

Hop, H., and Gjosaeter, H. (2013). Polar cod (*Boreogadus saida*) and capelin (*Mallotus villosus*) as key species in marine food webs of the Arctic and the Barents Sea. Mar. Biol. Res. *9*, 878–894.

Houde, E. (2008). Emerging from Hjort's shadow. J. Northwest Atl. Fish Sci. *41*, 53–70.

Incardona, J.P. (2017). Molecular mechanisms of crude oil developmental toxicity in fish. Arch. Environ. Contam. Toxicol. *73*, 19–32.

Incardona, J.P., Carls, M.G., Holland, L., Linbo, T.L., Baldwin, D.H., Myers, M.S., Peck, K.A., Rice, S.D., and Scholz, N.L. (2015). Very low embryonic crude oil exposures cause lasting cardiac defects in salmon and herring. Sci. Rep. *5*, 13499.

Incardona, J.P., Gardner, L.D., Linbo, T.L., Brown, T.L., Esbaugh, A.J., Mager, E.M., Stieglitz, J.D., French, B.L., Labenia, J.S., Laetz, C.A., et al. (2014). Deepwater horizon crude oil impacts the developing hearts of large predatory pelagic fish. Proc. Natl. Acad. Sci. U S A *111*, E1510–E1518.

Incardona, J.P., and Scholz, N.L. (2016). The influence of heart developmental anatomy on cardiotoxicity-based adverse outcome pathways in fish. Aquat. Toxicol. *177*, 515–525.

Incardona, J.P., and Scholz, N.L. (2018). Chapter 10: case study: the 2010 deepwater horizon oil spill. In Development, Physiology, and Environment, A. Synthesis, W.W. Burggren, and B. Dubansky, eds. (Springer), pp. 235–283.

Incardona, J.P., Vines, C.A., Linbo, T.L., Myers, M.S., Sloan, C.A., Anulacion, B.F., Boyd, D., Collier, T.K., Morgan, S., Cherr, G.N., et al. (2012). Potent phototoxicity of marine bunker oil to translucent herring embryos after prolonged weathering. PLoS One *7*, e30116.

Jeffries, M., Richter-Menge, J., and Overland, J. (2018). Arctic Report Card 2018 https://www.nps.gov/articles/arcticreportcard2018.htm.

Laurel, B., Spencer, M., Iseri, P., and Copeman, L. (2016). Temperature-dependent growth and behavior of juvenile Arctic cod (*Boreogadus saida*) and co-occurring North Pacific gadids. Polar Biol. *39*, 1127–1135.

Koenker, B.L., Laurel, B.J., Copeman, L.A., and Ciannelli, L. (2018). Effects of temperature and food availability on the survival and growth of larval Arctic cod (*Boreogadus saida*) and walleye pollock (*Gadus chalcogrammus*). ICES J. Mar. Sci. *75*, 2386–2402.

Laurel, B.J., Copeman, L.A., Spencer, M., and Iseri, P. (2018). Comparative effects of temperature on rates of development and survival of eggs and yolk-sac larvae of Arctic cod (*Boreogadus saida*) and walleye pollock (*Gadus chalcogrammus*). ICES J. Mar. Sci. *75*, 2403–2412.

Laurel, B.J., Hurst, T.P., and Ciannelli, L. (2011). An experimental examination of temperature interactions in the match-mismatch hypothesis for Pacific cod larvae. Can. J. Fish. Aquat. Sci. *68*, 51–61.

Laurel, B.J., Hurst, T.P., Copeman, L.A., and Davis, M.W. (2008). The role of temperature on the growth and survival of early and late hatching Pacific cod larvae (*Gadus macrocephalus*). J. Plankton Res. *30*, 1051–1060.

Mazeaud, M.M., Mazeaud, F., and Donaldson, E.M. (1977). Primary and secondary effects of stress in fish: some new data with a general review. Trans. Am. Fish. Soc. *106*, 201–212.

Morris, J.M., Gielazyn, M., Krasnec, M.O., Takeshita, R., Forth, H.P., Labenia, J.S., Linbo, T.L., French, B.L., Gill, J.A., Baldwin, D.H., et al. (2018). Crude oil cardiotoxicity to red drum embryos is independent of oil dispersion energy. Chemosphere *213*, 205–214.

Mueter, F.J., Nahrgang, J., John Nelson, R., and Berge, J. (2016). The ecology of gadid fishes in the circumpolar Arctic with a special emphasis on the polar cod (*Boreogadus saida*). Polar Biol. *39*, 961–967.

Nahrgang, J., Dubourg, P., Frantzen, M., Storch, D., Dahlke, F., and Meador, J.P. (2016). Early life stages of an arctic keystone species (*Boreogadus saida*) show high sensitivity to a water-soluble fraction of crude oil. Environ. Pollut. *218*, 605–614.

Nordtug, T., Olsen, A.J., Altin, D., Meier, S., Overrein, I., Hansen, B.H., and Johansen, O. (2011). Method for generating parameterized ecotoxicity data of dispersed oil for use in environmental modelling. Mar. Pollut. Bull. *62*, 2106–2113.

Parrish, C.C. (1988). Dissolved and particulate marine lipid classes - a review. Mar. Chem. *23*, 17–40.

Peck, M., and Moyano, M. (2016). Measuring respiration rates in marine fish larvae: challenges and advances. J. Fish Biol. *88*, 173–205.

Peterson, C.H., Rice, S.D., Short, J.W., Esler, D., Bodkin, J.L., Ballachey, B.E., and Irons, D.B. (2003). Long-term ecosystem response to the Exxon Valdez oil spill. Science *302*, 2082–2086.

Rice, S.D., Thomas, R.E., Carls, M.G., Heintz, R.A., Wertheimer, A.C., Murphy, M.L., Short, J.W., and Moles, A. (2001). Impacts to pink salmon following the Exxon Valdez oil spill: persistence, toxicity, sensitivity, and controversy. Rev. Fish Sci. *9*, 165–211.

Siddon, E.C., Heintz, R.A., and Mueter, F.J. (2013). Conceptual model of energy allocation in walleye pollock (*Theragra chalcogramma*) from age-0 to age-1 in the southeastern Bering Sea. Deep Sea Res. II *94*, 140–149.

Sogard, S.M. (1997). Size-selective mortality in the juvenile stage of teleost fishes: a review. Bull. Mar. Sci. *60*, 1129–1157.

Sogard, S.M., and Olla, B.L. (2000). Endurance of simulated winter conditions by age-0 walleye pollock: effects of body size, water temperature and energy stores. J. Fish Biol. *56*, 1–21.

Sørensen, L., Sørhus, E., Nordtug, T., Incardona, J.P., Linbo, T.L., Giovanetti, L., Karlsen, O., and Meier, S. (2017). Oil droplet binding and differential PAH toxicokinetics in embryos of Atlantic haddock and cod. PLoS One *12*, e0180048.

Sørhus, E., Incardona, J.P., Furmanek, T., Goetz, G.W., Scholz, N.L., Meier, S.,

Edvardsen, R.B., and Jentoft, S. (2017). Novel adverse outcome pathways revealed by chemical genetics in a developing marine fish. Elife *6*, e20707.

Sørhus, E., Incardona, J.P., Karlsen, Ø., Linbo, T.L., Sørensen, L., Nordtug, T., van der Meeren, T., Thorsen, A., Thorbjørnsen, M., Jentoft, S., et al. (2016). Effects of crude oil on haddock reveal roles for intracellular calcium in craniofacial and cardiac development. Sci. Rep. *6*, 31058.

Timmermans, M.L., and Proschutinsky, A. (2014). Arctic ocean sea surface temperature. Arctic Report Card 2014 https://www.arctic.noaa.gov/Portals/7/ArcticReportCard/Documents/ArcticReportCard_full_report2014.pdf.

Tocher, D.R. (2003). Metabolism and functions of lipids and fatty acids in teleost fish. Rev. Fish. Sci. *11*, 107–184.

Vihtakari, M., Welcker, J., Moe, B., Chastel, O., Tartu, S., Hop, H., Bech, C., Descamps, S., and Gabrielsen, G.W. (2018). Black-legged kittiwakes as messengers of atlantification in the Arctic. Sci. Rep. *1178*, 1–11.

ISCI, Volume *19*

Supplemental Information

Embryonic Crude Oil Exposure Impairs Growth and Lipid Allocation in a Keystone Arctic Forage Fish

Benjamin J. Laurel, Louise A. Copeman, Paul Iseri, Mara L. Spencer, Greg Hutchinson, Trond Nordtug, Carey E. Donald, Sonnich Meier, Sarah E. Allan, Daryle T. Boyd, Gina M. Ylitalo, James R. Cameron, Barbara L. French, Tiffany L. Linbo, Nathaniel L. Scholz, and John P. Incardona

Transparent Methods

Polar cod husbandry and spawning. Polar cod is a circumpolar, cold-adapted pelagic marine fish that spawns under or near-ice in winter and spring (Bouchard and Fortier, 2011). Eggs are buoyant and relatively large for a gadid (1.8 mm). Developments times are protracted – e.g., ~45 days at 2°C (Laurel et al., 2018). Larvae are ~6.0 mm standard length (SL) at hatch, undergo flexion between 8-12 mm SL and gradually transition to pelagic juvenile stages through the summer 20- 50 mm SL before their first overwintering period (Bouchard and Fortier, 2011; Koenker et al., 2018; Laurel et al., 2017). Here, fertilized eggs were obtained from a captive broodstock consisting of 27 F_1-generation adults (21 females, 6 males) held at the NOAA Alaska Fisheries Science Center laboratory at the Hatfield Marine Science Center in Newport, OR. The F_o for these fish were collected as juveniles from the Beaufort Sea (Prudhoe Bay, AK, 70.383°N -148.552°W) and transported to the Hatfield facility in 2012. Adults were held at 2 °C and individuals were non-lethally strip spawned on Feb. 24, 2017 to produce two discrete egg batches, each derived from a single female fertilized with milt from three males. The two batches were combined and incubated at 2°C in static 38-L aquaria held in cold rooms with a 20% daily water exchange prior to the onset of oil exposure (described below). At the point during embryogenesis when the heart first began to beat (21 dpf), an equal volume of embryos (8 ml) was introduced to four replicate containers (~ 1400 eggs/container) for each of four oil exposure treatments (0, 100, 300 and 900 µg nominal oil by mass/L; n = 16 total containers). In all aspects of the study, animals were cared for in accordance with the policies of the U.S. Department of Commerce and the Public Health Service, conforming to the standards of the National Academy of Sciences' Guide for the Care and Use of Laboratory Animals (Council, 2011).

Oil exposures. Alaska North Slope crude oil, collected at the terminus of the Trans-Alaska pipeline in 2014 was used for this study. The Alaska North Slope pipeline blend is a medium-gravity (29.8° API) crude oil that originates from multiple production fields in Prudhoe Bay. Prior to the exposures, the oil was artificially weathered by distillation to emulate the rapid loss of relatively volatile, monoaromatic compounds and lower molecular weight PAHs that normally occurs following a release of oil at sea. The weathered oil was mechanically dispersed using a syringe pump to drive oil continuously through a droplet generator (Nordtug et al., 2011) at a rate of 45 µL/hour. The oil dispersion was then mixed with seawater from a pump at 180 mL/min (Fig. S1A). A computer-controlled solenoid valve manifold distributed different ratios of dispersed oil and clean seawater (33 ppt) to 2.4-L glass exposure vessels nested in temperature-controlled water baths holding fish embryos (Fig. S1B). Relative to conventional methods (e.g., oiled gravel columns), the computer-driven dispersion generator produces a more precise and reproducible delivery of oil droplets to exposure chambers for marine fish embryos (Nordtug et al., 2011). As noted above, the treatments included control (clean seawater) and low (100 µg nominal mass of oil/L), medium (300 µg/L) and high (900 µg/L) exposures. Oil dispersion was delivered to each of the replicate exposure tanks at a flow rate of 12 mL/min. To differentiate between oil exposures in the water column and those proximal to surface slicks, a subset of embryos was held below the surface in 500 µm mesh containers for each replicate (Fig. S1C). Oil delivery was terminated after 72 h of exposure, after which all of the embryos in the submerged chambers and a subsample of embryos at the surface were collected for tissue chemistry and the quantitation of *cyp1a* gene expression (described below). The remaining surface embryos were held in the exposure chambers for an additional 4 day washout period and

then rinsed in clean seawater and transferred to new 12 L containers in a 2°C cold room. Cod were maintained in these containers until hatching at 50 dpf, and dead embryos were siphoned from each container and counted daily.

Larval and juvenile growth in clean seawater. After hatching (50 dpf), yolk-sac Polar cod larvae from cold rooms were transferred in 1-L beakers to a series of black, conical upwelling tanks (45 L) corresponding with each replicate treatment (n = 16 tanks total). Each acclimation tank was supplied with flow-through, temperature-controlled seawater at 2°C. Larvae were stocked at a density of 600 individuals per tank. Tanks were placed on a 12:12 hr light:dark photoperiod with daily light intensity ranging from 2.4 – 2.7 $\mu E/m^2 sec$ at the surface of the water in the center of each tank. Tank temperatures, aeration, and flow rates were monitored daily, and each was siphoned twice weekly to remove any mortalities along with excess food and debris. Larvae were pulse fed enriched rotifers (*Brachionus* sp.) twice daily at a density of 5 prey/mL. At 10 weeks, enriched brine shrimp (*Artemia* sp.) were added to the diet at a prey density of 2 prey/mL. At 14 weeks, the larvae were switched to a commercial dry particulate food (Otohime a/B1) augmented with brine shrimp. Prior to each feeding, Nanno 3600 algae paste (Reed Mariculture, Campbell, CA, USA) diluted with 2 °C seawater was added to each tank to improve the feeding environment (Naas et al., 1992).

PAH measurements in water and tissues. All individual PAH measures for water and tissue are provided in Database S1. Water samples (200 mL) for PAH measures were collected directly from the exposure tank inlet capillaries at exposure start (day 0) and at day 3, and from the tank water column at exposure days 1, 3, and 7 for each replicate. Samples were stabilized by the addition of 20 mL dichloromethane and stored at 4ºC until extraction and analysis. After addition

of internal standards, water samples were extracted with dichloromethane and analyzed using GC/MS selected ion monitoring with additional monitoring for alkylated PAHs as detailed elsewhere (Sloan et al., 2014). A PAH-spiked water blank and a method blank sample were analyzed concurrently with samples. The lower limits of quantification for PAHs ranged from <0.0017 to <0.0086 ng/L. Values for ∑PAHs in the text include all measured values above the detection limits.

Samples of 100 viable embryos were collected from each replicate (n=4) tank and incubation position (floating and submerged) at the multiple time periods during exposure (See Figure S1) and preserved with flash-freezing. Body burden samples were extracted using the miniaturized extraction techniques detailed elsewhere (Sorensen et al., 2016). Samples were homogenized with a microprocessor (Virtis Tempest IQ 2.0) in 2 mL *n*-hexane and dichloromethane (v/v, 1:1) after adding internal standards. Samples were vortexed with 200 mg sodium sulphate as a drying agent and centrifuged, and the supernatant was collected before repeating twice. After concentrating under N_2 to 1 mL, the samples were cleaned-up using Agilent Bond Elut SI, 500 mg (Agilent Technologies USA) eluted with 6 mL *n*-hexane and dichloromethane (v/v, 9:1). Samples were then reduced under N_2 to 100 µL. Blank samples containing no eggs were included in each daily batch. Analysis was performed using an Agilent 7890 gas chromatograph coupled to an Agilent 7010 triple quadrupole mass spectrometer (Sorensen et al., 2016). As confirmation of performance, 80% of target compounds were within 25% deviation of known values.

Live imaging for morphological and functional defects. Embryos and larvae were mounted in 3% methylcellulose in seawater and imaged on Nikon SMZ800N LED-illuminated stereoscopes

in a cold room at 2ºC. Digital videos and still images were acquired with Unibrain Fire-i780c 1394 cameras (unibrain.com) connected via firewire to Apple laptop computers with the BTV Pro application (Bensoftware.com). Prior to mounting, larval stages were anesthetized in Petri dishes with a dose of MS-222 (50 g/L stock) that was titrated to just stop swimming activity. At all stages, animals were randomly selected from either the surface (egg stages) or captured from the water column via a large bore pipet. Random subsamples of embryos were imaged during the exposure to assess interaction with oil droplets, starting with a pre-exposure sample and then at exposure days 1, 3, and 5. On exposure day 3, both surface and submerged embryos were imaged. Quantification of oil droplets bound to surface-exposed embryos at exposure day 3 was performed by manually counting droplets in representative images using the Multi-point tool in ImageJ (ImageJ.nih.gov/ij/). For assessing cardiac morphology and function, 30-sec videos were recorded for each fish at the highest magnification (8x), focusing on the cardiac/pericardial region in left-lateral views. Low magnification images of the entire larva were collected for each for morphometrics, as well as representative higher magnification composites. Cardiac data were collected for 10 embryos from each replicate (160 total) at the end of exposure (day 7), 30 per replicate for newly hatched yolk sac larvae (480 total), and 5 per replicate at 43 dph (60 total; high treatment had no survivors at this point),

Pericardial edema was scored in digital videos of hatched yolk sac larvae by observing whether the pericardial membranes contacted the cardiac chambers. Heart rate was determined by manually counting the number of contractions in each video collected at all time points. Rhythm irregularity was quantified at the end of exposure using a region of interest (ROI) plugin developed for ImageJ. ROIs were traced on the atrial chamber, and data output from each video frame was plotted in Microsoft Excel. Peaks for each atrial contraction were identified manually

and entered into Excel, then differences calculated and averaged to produce the minimum and maximum contraction time (beat duration and interbeat range) for each animal. Due to motion artifacts, not all movies were used in this analysis, which included at least 6/10 from each replicate. Ventricular shape was assessed in digital videos of 43 dph larvae by freehand tracing the ventricle and using the shape descriptors measurements in ImageJ.

Quantification of *cyp1a* gene expression. For each exposure tank, a sample of 20 embryos was collected at both the surface and from the submerged container and flash frozen in liquid nitrogen prior to storage at -80 °C. Total RNA was extracted by homogenizing samples in TRIzol (5% v/v, ThermoFisher Scientific, Waltham, MA) and then purified with a Direct-zol™ RNA MiniPrep column (Zymo Research, Irvine, CA; #R2052). RNA concentrations and purity were measured using a Nanodrop ND-1000 Spectrophotometer. Superscript IV (Thermofisher Cat #18090050) with oligo dT(20) primers was used to synthesize cDNA.

Reverse transcriptase quantitative polymerase chain reaction (RT-qPCR) was performed on a Viia™ 7 Real-Time PCR system (Applied Biosytems/ThermFisher Scientific) with a 384-well block using Fast SYBR Green (ThermoFisher Scientific). Gene-specific RT-qPCR primers are shown below:

	Forward	Reverse
ef1a	GTCATCATCCTGAACCACCCTG	AACGGTCTGCCTCATGTCAC
cyp1a	CCACCCCGAGATGCAGG	CGAAGGTGTCTTTGGGGA
rxrba	GCARATGGACAARACWGAGC	AAMGTGTCRATAGGBGTGTC

Primers were designed using Primer3 (http://bioinfo.ut.ee/primer3/) and synthesized by Integrated DNA Technologies, Inc. (Skokie, Illinois), except for *cyp1a*, which is previously published (Nahrgang et al., 2009). Primers for *ef1a* were designed by targeting identical regions between the *G. morhua* (GenBank DQ402371.1) and *Oncorhynchus mykiss* (GenBank NM_001124339.1) *ef1a* genes. The design of degenerate primers for *rxrba* was based on the consensus sequence derived from the alignment of homologues from four different teleost families. Each 10-µl reaction was formulated with Fast SYBR™ Master Mix (Cat No. 4385617) as specified by the manufacturer, in duplicate for each biological replicate. Each reaction contained an estimated 10 ng of sample cDNA and 500 nM of each primer. Reactions were cycled 40 times from 95 ºC for 15 seconds to and annealing temperature of 60 ºC for 20 seconds.

Reference genes *ef1a*, and *rxrba* were analyzed and selected by a consensus of BestKeeper, GeneNorm, and NormFinder algorithms using RefFinder, a free online software (Xie et al., 2012). Due to the low RNA yield of samples, primer efficiency was measured using standard curves generated from cDNA from the same cohort rather than from cDNA from experimental samples. Primer efficiencies and r^2 were within acceptable range (>90%; Nolan et al., 2006). Degenerate primers for *rxrba* amplified a single product. All qPCR products were sequenced and found to correspond to target genes. The *cyp1a* product was identical to that previously published (GenBank ID EU682947.1; Nahrgang et al., 2009). Sequences for Polar cod *ef1a* and *rxrba* were deposited in GenBank (MN265824 and MN265825, respectively). Normalized Cq values (dCq) and relative fold-change values were calculated using the Comparative Ct method (Schmittgen and Livak, 2008).

Lipid measurements. Lipid samples were collected on the first day of the embryonic exposure (20 dpf, n = 3 replicates, 50 individuals per replicate), at the end of the washout period (27 dpf, n = 3, 50/replicate), at hatch (45 dpf, n = 6, 50/replicate) and during four additional grow-out time points (66 dpf, n = 3, 50/replicate; 86 dpf, n = 3, 10/replicate; 121 dpf, n = 3, 3/replicate; and 156 dpf, n = 3, 5/replicate). The grow-out was terminated at 191 dpf, at which point 32 and 20 individuals were collected from the control and low treatments, respectively, with each individual constituting a distinct replicate. The above variation in sample numbers reflects a balance between the need for a minimum of 500 µg lipid per replicate and enough remaining fish for the grow-out. All lipids statistics are reported as tank mean as the unit of replication with 1-2 samples per tank except at 191 dpf, when 8-16 individuals were analyzed per tank.

Lipids were extracted in chloroform and methanol quantified using thin layer chromatography with flame ionization detection (TLC-FID) with a MARK VI Iatroscan (Iatron Laboratories, Tokyo, Japan) as previously described (Copeman et al., 2016; Lu et al., 2008). Lipid classes were separated on silica-coated Chromarods with a three-stage development system (56), scanned using PeakSimple software (ver. 3.67, SRI Inc.) and quantified using lipid standards (59). Resulting chromatograms were integrated to quantify absolute amounts of triacylglycerols, free fatty acids, sterols, and polar lipids, calculated as the average of triplicate runs for each sample.

Gross morphology and growth. Morphometry was performed at hatch (dry mass, standard length, myotome height, eye diameter) and multiple times post-hatch (mass and length only; Fig. S1). Larvae were anesthetized with MS-222 (50 g/L) and individual images were taken under calibrated magnification using a digital camera attached to a stereomicroscope. Digital images

were collected using ImagePro® software (Media Cybernetics, Bethesda, MD, USA). From these, standard length was measured from the tip of the rostrum to the posterior end of the notochord and myotome height measured posterior to the anus. Following imaging, fish were rinsed with a 3% ammonium formate solution to remove excess salts and placed on pre-weighed aluminum foil squares. Foil squares were then folded securely and placed in labelled slots on a baking sheet in a drying oven. Samples were dried at 55°C for a minimum of 48 hours before determination of dry mass with a microbalance (Sartorius R16OP) to the nearest 1.0 µg. All dry mass data are reported as µg/individual.

Data Analysis. Data were analyzed in SYSTAT software (version 12; SYSTAT) or JMP13 (SAS, Cary, NC) using tank means. Hatch success (%), larval size-at-hatch (SL), eye diameter, myotome height, time-to-hatch (50%), and lipid content at hatch (µg per larvae) were tested using analysis of variance (ANOVA) with oil exposure as a fixed factor and Tukey's multiple comparison. Cardiac data were analyzed by ANOVA with post-hoc means comparisons by Dunnett's test. Analysis of latent impacts on lipid density (µg/g) and size (DWT) was also analyzed by ANOVA at each sampling period following hatch. Expression levels of *cyp1a* mRNA were analyzed by 1- or 2-parameter regression. All data were checked for normality and homoscedasticity to meet the assumptions of each statistical model.

Table S1: ∑PAHs (µg/L) in water measured throughout the exposure period in the experimental timeline (see Figure S1). For reference, Day 0 refers to 21 days post-fertilization (dpf) in Fig. S1D. Values represent mean ± s.e.m. for the four replicate tanks.

nominal oil load	Day 0 inlet	Day 3 inlet	Day 1 water column	Day 3 water column	Day 7 water column
control	0.054 ± 0.002	0.044 ± 0.005	0.109 ± 0.014	nd	0.050 ± 0.001
100 ug/L	1.5 ± 0.2	2.7 ± 0.5	0.65 ± 0.20	1.1 ± 0.1	0.19 ± 0.05
300 ug/L	8.3 ± 0.6	13.0 ± 0.4	2.6 ± 0.3	4.0 ± 0.1	0.43 ± 0.14
900 ug/L	25.8 ± 2.8	53.3 ± 8.3	11.9 ± 2.3	18.3 ± 2.7	1.7 ± 0.4

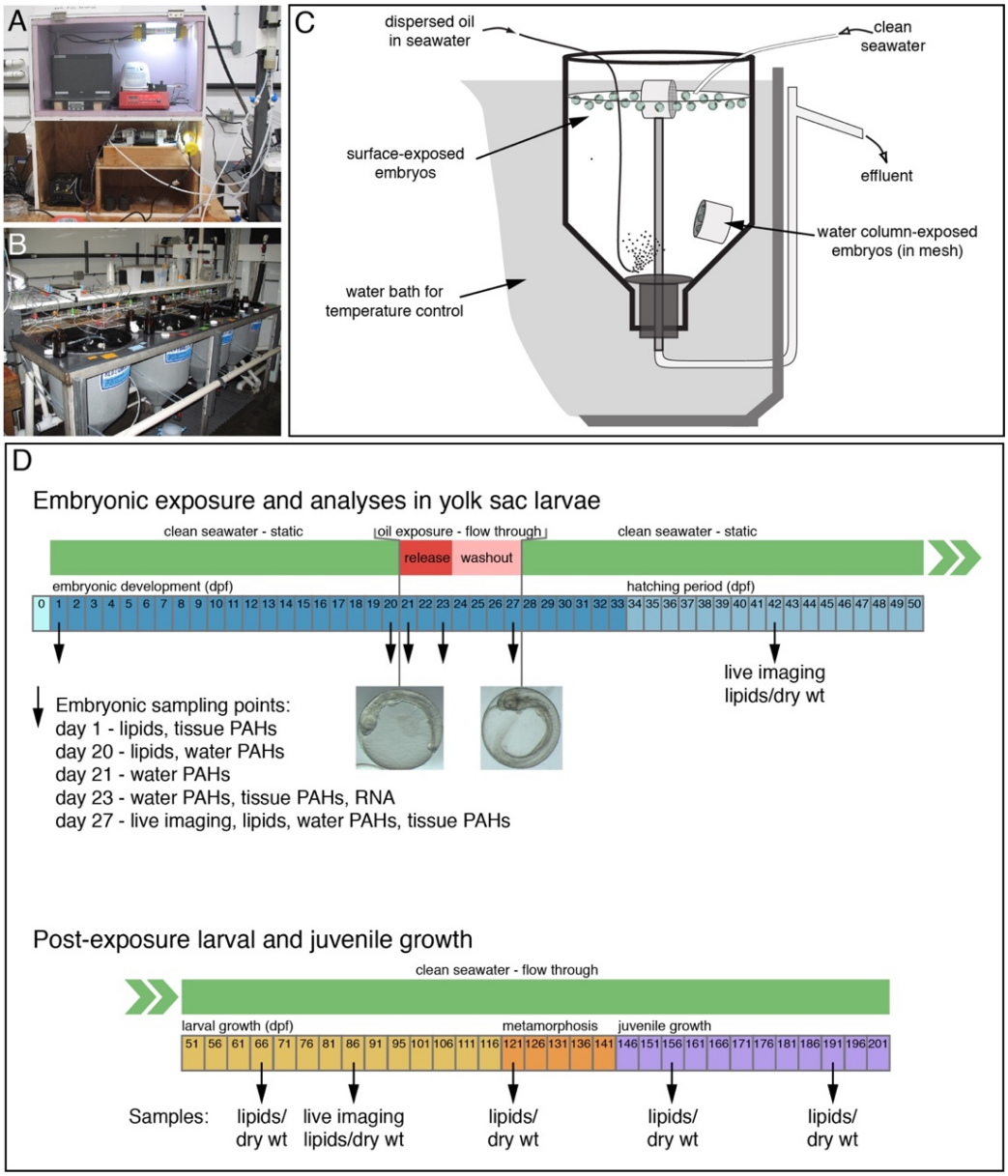

Figure S1. Overview of the oil dispersion system and experimental design. (A) Oil was mechanically dispersed with a syringe pump driving oil continuously through a dispersion droplet generator at a rate of 45 □L/hour, which was mixed with seawater from a pump at 180 mL/min. (B) Dispersed oil and clean seawater were distributed by a computer-controlled solenoid valve manifold distributed different ratios of dispersed oil and clean seawater (33 ppt) above a series of 8 temperature-controlled water baths. (C) Dispersed oil concentrations were delivered to glass exposure vessels nested in temperature-controlled water baths holding fish embryos at and below the water surface. (D) Analytical chemical analyses and endpoint measurements (lipid, imaging, RNA) were conducted at multiple time periods during and after oil-exposure. The experiment was terminated at 193 days post fertilization.

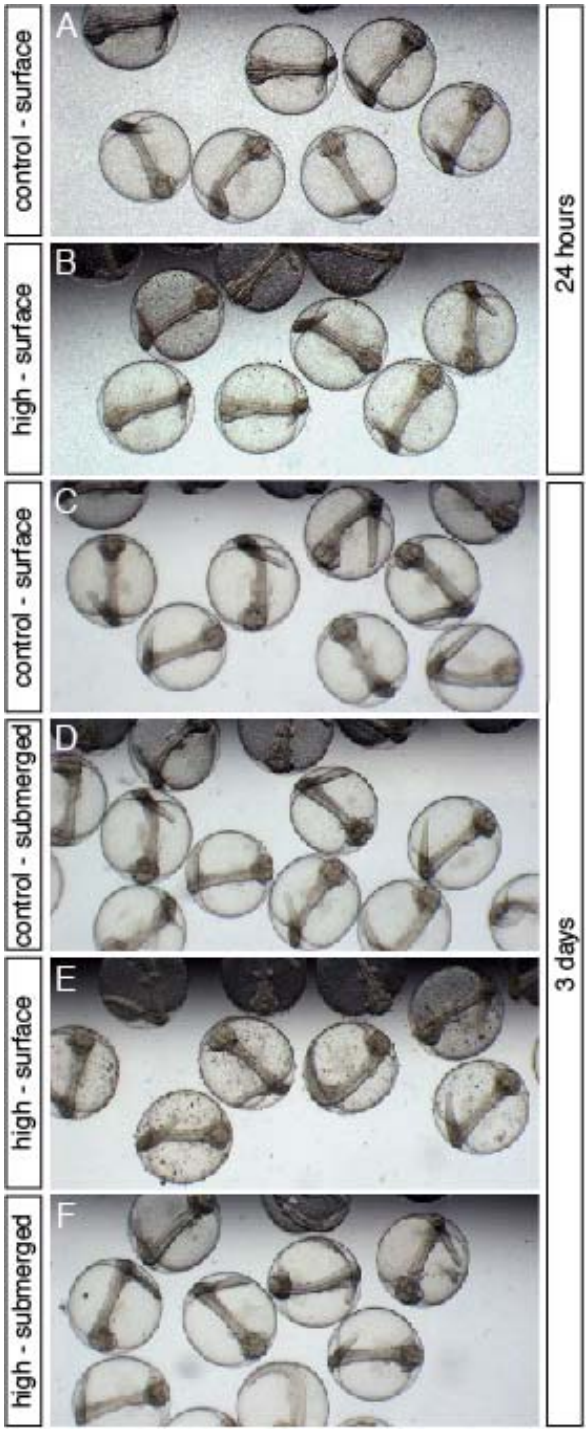

Figure S2. Adherence of oil microdroplets to the chorions of surface-oriented Polar cod embryos. Clean control embryos (A) and embryos from the surface of the high exposure (B) with adherent droplets after 24 hours of oil release. Control surface (C) and submerged embryos (D) are compared to surface (E) and submerged (F) embryos from the high exposure after 3 days of oil release.

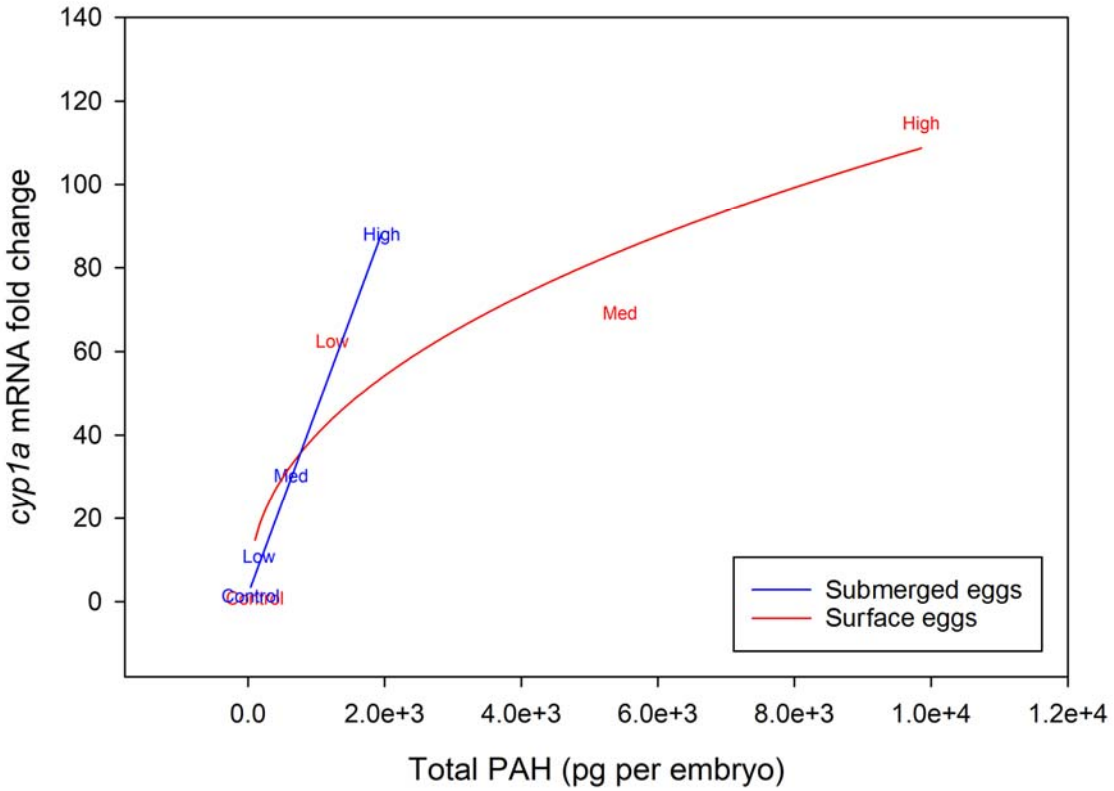

Figure S3. The relative expression of *cyp1a* in relation to total polycyclic aromatic hydrocarbons (PAHs) in the tissues of cod embryos was strongly influence by vertical distribution in the water column. Whereas *cyp1a* upregulation was linear for submerged embryos (*cyp1a=1.75+0.044*PAH*; $r^2 = 0.997$) buoyant embryos at the surface had relatively higher body burdens of PAHs per treatment with a corresponding expression of *cyp1a* that was non-linear ($cyp1a=1.965*PAH^{0.4967}$; $r^2 = 0.879$). Data for figure are reported in Table 1.

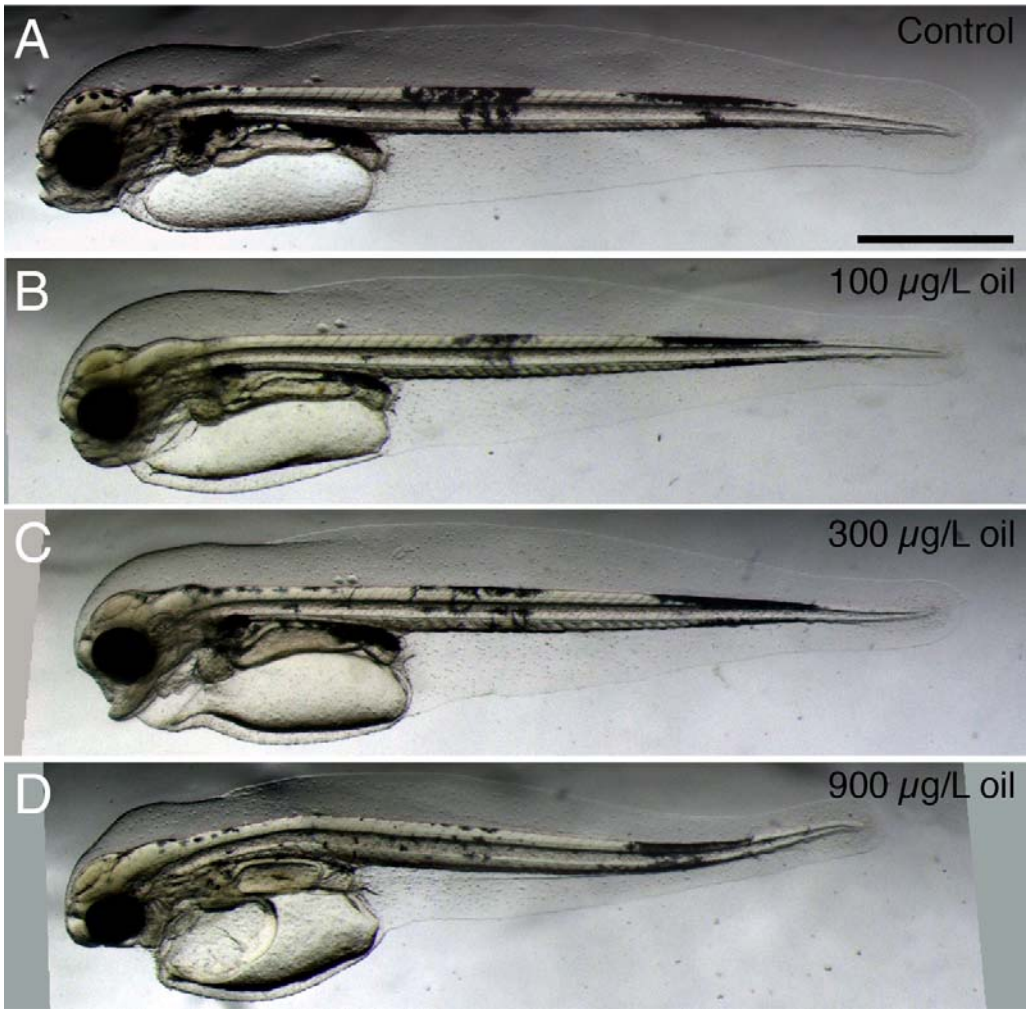

Figure S4. Gross morphology of representative hatching stage yolk sac larvae from control (A), low (B), medium (C) and high (D) exposure groups. Scale bar = 1 mm.

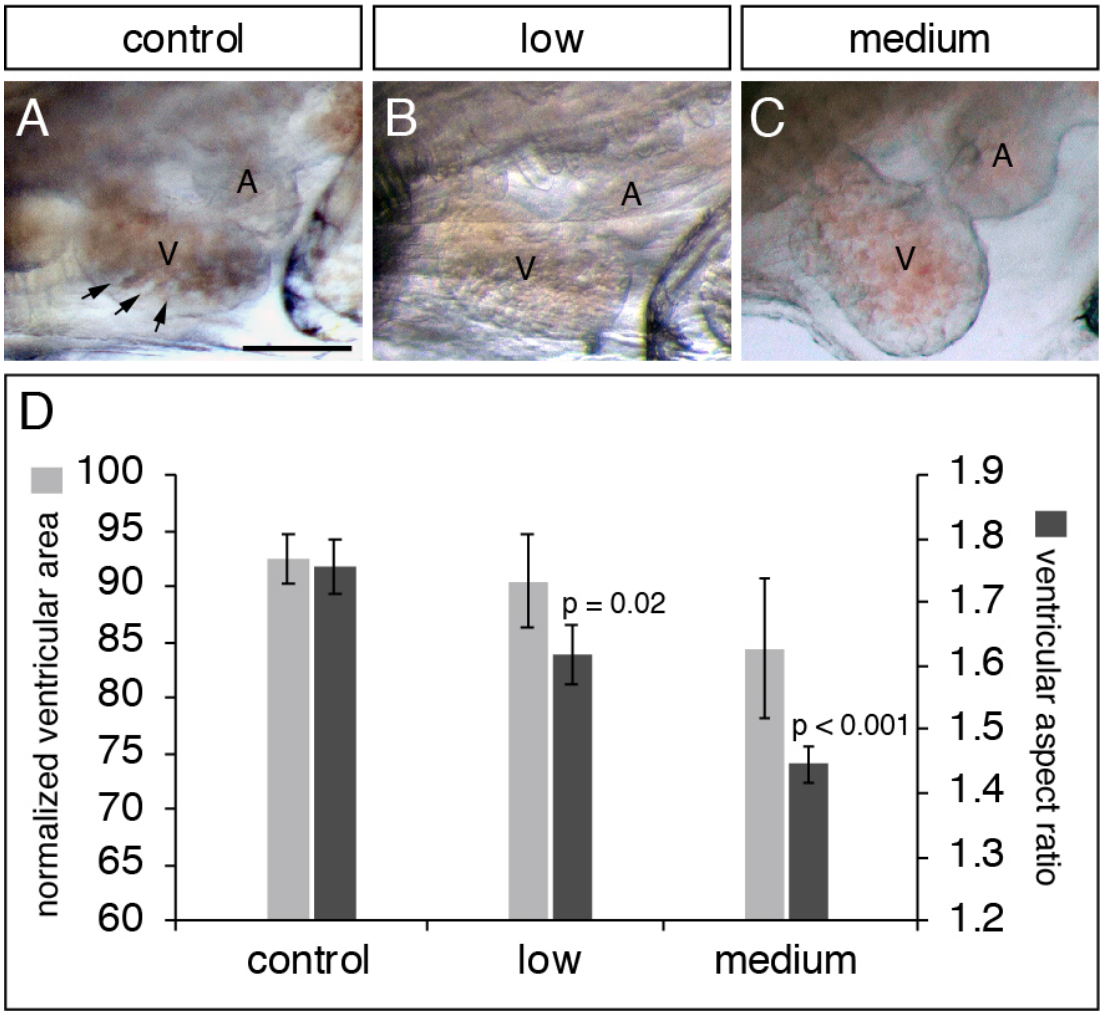

Figure S5. Persistent defects in cardiac morphology at 43 days post hatch (86 dpf). (A – C) Representative lateral views of larval hearts during ventricular diastole (anterior to the left and dorsal at top). (A) Control larva and larva from (B) low and (C) medium exposure groups. *V*, ventricle; *A*, atrium; arrows indicated trabeculae in control. Scale bar is 50 µm. (D) Diastolic ventricular area normalized to fish standard length (left y-axis) and aspect ratio (right y-axis) taken from lateral view videos. Values are means (±SEM) for 5 larvae from each of 4 replicate tanks.

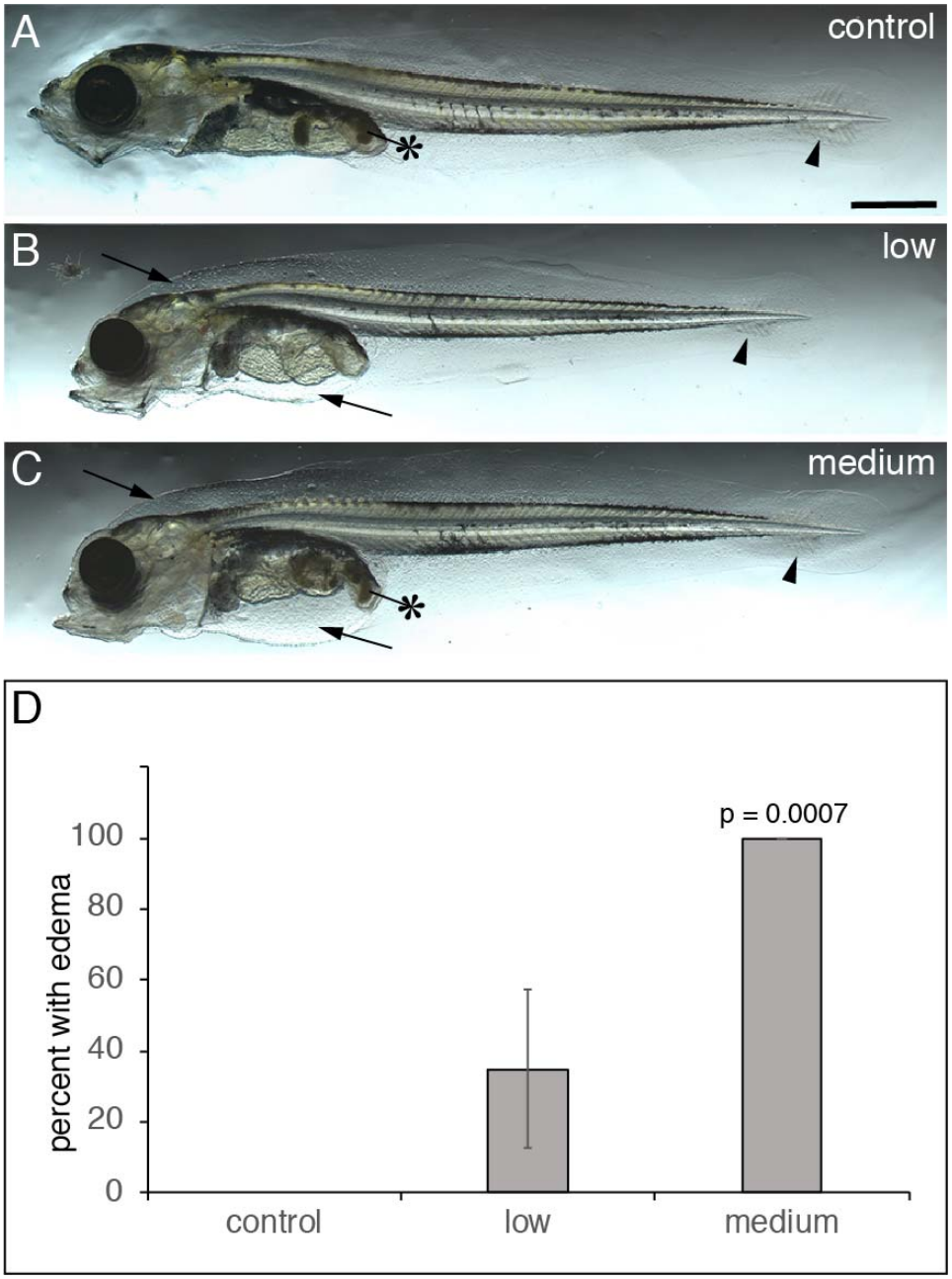

Figure S6. Persistent dose-dependent edema at 43 days post hatch (86 dpf). Representative larval morphology for (A) control, (B) low, and (C) medium exposure groups. Arrows indicate edema fluid accumulation evident as ascites around the gut and retention of the dorsal subdermal space above the brain in (B) and (C). Arrowheads indicate the developing caudal fin rays, which were roughly coincident in each treatment group. Asterisks indicate food in the gut. Scale bar is 1 mm. (D) Quantification of the presence of edema, based on images of 5 randomly selected larvae from each of 4 replicate tanks. Values are means (±SEM) p value derived from ANOVA and Dunnett's test post-hoc.

Supplemental Item Captions:

Movie S1. Ectopic pacemaker and retrograde contraction from the atrioventricular region in Polar cod embryos immediately after oil exposure. A pair of 30-sec video clips show the beating looping-stage heart for representative embryos from control and high dose (900 µg/L oil) exposures. Embryos are viewed ventrally through the chorion with the atrium (*A*) oriented to the video's right and ventricle (*V*) near the midline. *AVC*, atrioventricular canal.

External Database S1. Detailed measurements for individual PAHs from all water and tissue samples.

References

Bouchard, C., and Fortier, L. (2011). Circum-arctic comparison of the hatching season of polar cod *Boreogadus saida*: A test of the freshwater winter refuge hypothesis. Prog Oceanogr *90*, 105-116.

Copeman, L.A., Laurel, B.J., Boswell, K.M., Sremba, A.L., Klinck, K., Heintz, R.A., Vollenweider, J.J., Helser, T.E., and Spencer, M.L. (2016). Ontogenetic and spatial variability in trophic biomarkers of juvenile saffron cod (*Eleginus gracilis*) from the Beaufort, Chukchi and Bering Seas. Polar Biology *39*, 1109-1126.

Koenker, B.L., Laurel, B.J., Copeman, L.A., and Ciannelli, L. (2018). Effects of temperature and food availability on the survival and growth of larval Arctic cod (*Boreogadus saida*) and walleye pollock (*Gadus chalcogrammus*). ICES J Mar Sci, fsy062-fsy062.

Laurel, B.J., Copeman, L.A., Spencer, M., and Iseri, P. (2017). Temperature-dependent growth as a function of size and age in juvenile Arctic cod (*Boreogadus saida*). ICES J Mar Sci *74*, 1614–1621.

Laurel, B.J., Copeman, L.A., Spencer, M., Iseri, P., and Handling editor: Dominique, R. (2018). Comparative effects of temperature on rates of development and survival of eggs and yolk-sac larvae of Arctic cod (*Boreogadus saida*) and walleye pollock (*Gadus chalcogrammus*). ICES Journal of Marine Science, fsy042-fsy042.

Lu, Y.H., Ludsin, S.A., Fanslow, D.L., and Pothoven, S.A. (2008). Comparison of three microquantity techniques for measuring total lipids in fish. Canadian Journal of Fisheries and Aquatic Sciences *65*, 2233-2241.

Nahrgang, J., Camus, L., Gonzalez, P., Goksoyr, A., Christiansen, J.S., and Hop, H. (2009). PAH biomarker responses in polar cod (*Boreogadus saida*) exposed to benzo(a)pyrene. Aquat Toxicol *94*, 309-319.

Naas, K.E., N¶ss, T., and Harboe, T. (1992). Enhanced first feeding of halibut larvae (*Hippoglossus hippoglossus* L.) in green water. Aquaculture *105*, 143-156.

National Research Council, (2011). Guide for the Care and Use of Laboratory Animals, 8th edn (Washington, D. C.: National Academies Press)

Nolan, T., Hands, R.E., and Bustin, S.A. (2006). Quantification of mRNA using real-time RT-PCR. Nat Protoc *1*, 1559-1582.

Nordtug, T., Olsen, A.J., Altin, D., Meier, S., Overrein, I., Hansen, B.H., and Johansen, O. (2011). Method for generating parameterized ecotoxicity data of dispersed oil for use in environmental modelling. Mar Pollut Bull *62*, 2106-2113.

Schmittgen, T.D., and Livak, K.J. (2008). Analyzing real-time PCR data by the comparative C-T method. Nat Protoc *3*, 1101-1108.

Sloan, C.A., Anulacion, B.F., Baugh, K.A., Bolton, J.L., Boyd, D., Boyer, R.H., Burrows, D.G., Herman, D.P., Pearce, R.W., and Ylitalo, G.M. (2014). Northwest Fisheries Science Center's analyses of tissue, sediment, and water samples for organic contaminants by gas chromatography/mass spectrometry and analyses of tissue for lipid classes by thin layer chromatogrphy/flame ionization detection. In NOAA Technical Memorandum, pp. 61

Sørensen, L., Meier, S., and Mjos, S.A. (2016). Application of gas chromatography/tandem mass spectrometry to determine a wide range of petrogenic alkylated polycyclic aromatic hydrocarbons in biotic samples. Rapid Commun Mass Sp *30*, 2052-2058.

Xie, F.L., Xiao, P., Chen, D.L., Xu, L., and Zhang, B.H. (2012). miRDeepFinder: a miRNA analysis tool for deep sequencing of plant small RNAs. Plant Mol Biol *80*, 75-84.